Sleep-Stage Decision Algorithm by Using Heartbeat and Body-Movement Signals

Yosuke Kurihara and Kajiro Watanabe, *Member, IEEE*

***Abstract*—This paper describes a noninvasive algorithm to estimate the sleep stages used in the Rechtschaffen and Kales method (R–K method). The heartbeat and body-movement signals measured by the noninvasive pneumatic method are used to estimate the sleep stages instead of using the Eletroencephalogram and Electromyography in the R–K method. From the noninvasive measurements, we defined two indices that indicate the condition of REM sleep and the sleep depth. Functions to obtain the incidence ratio and the standard deviation of the extracted elements for each sleep stage were also determined, for each age group of the subjects. Using these indices and functions, an algorithm to classify the subjects' sleep stages was proposed. The mean agreement ratios between the sleep stages' data obtained from the proposed method and those from the de facto standard R–K method, for the stages categorized into six, five, and three, were 51.6%, 56.2%, and 77.5%, and their corresponding mean values of kappa statistics were 0.29, 0.39, and 0.48, respectively. The proposed method shows closer agreement with the result of R–K method than the similar noninvasive method presented earlier.**

***Index Terms*—Heartbeat, non REM stage, REM stage, sleep stage, unconstrained biomeasurement.**

I. Introduction

SLEEPING, which accounts for one-third of humans' lifetime, provides rest and comfort and also plays an important role in restoring the brain and the body from fatigue [1], [2]. As the ability to sleep well degrades with age and sleep loses its function to restore the brain and the body from fatigue, it becomes difficult to stay healthy. In Japan, where society is aging dramatically, promoting good health is an important national issue, and some administrative institutions are starting to address the matter [3]. Nightly monitoring of the transition of sleep quality at home is important for preserving good health and preventing sleep-related diseases, and so, unconstrained nightly monitoring of sleep conditions will be of great help.

Sleep conditions are now measured with the world standard Rechtschaffen and Kales method (R–K method) [4], which categorizes them into six stages, namely, Wake, REM stage, Sleep 1, Sleep 2, Sleep 3, and Sleep 4, based on brain waves, eye movement, and the Electromyography (EMG) of jaw muscle. This method, however, largely constrains body movement as it requires electrodes to be attached to the head, eyelids, and jaw in order to measure brain waves, eye movement, and the EMG of jaw muscle. The large size and high cost of the equipment also make the method impractical at home. There have been many research studies on the monitoring of sleep conditions [5]–[12], but all of them used noninvasive sensors attached to a bed to measure heartbeat, body movement, and other elements to estimate the sleep conditions. In contrast, we have developed an unconstrained pneumatic method to measure heartbeat and body movement and used it to estimate the sleep stages used for the R–K method [13]–[16]. The relation between the heartbeat spectrum and the sleep stages was also surveyed [17]. These methods and their results, however, still involved the following problems:

1) the same indices were used to examine REM and non-REM sleeps, which have different properties;
2) the precision of the sleep-stage estimation needs to be improved.

This paper proposes a method that solves these problems.

Manuscript received April 16, 2011; revised November 2, 2011; accepted January 13, 2012. Date of publication May 3, 2012; date of current version October 12, 2012. This paper was recommended by Associate Editor K. W. Hipel.

Y. Kurihara is with the Department of Computer and Information Science, Faculty of Science and Technology, Seikei University, Tokyo 180-8633, Japan (e-mail: yosuke-kurihara@st.seikei.ac.jp).

K. Watanabe is with the Department of Advanced Sciences, Faculty of Science and Engineering, Hosei University, Tokyo 184-8584, Japan.

Digital Object Identifier 10.1109/TSMCA.2012.2192264

II. Outline of Issues in This Paper

In this paper, we discuss the following issues to solve the problems mentioned earlier.

P-1: An index to indicate the REM sleep is defined.
P-2: An index to indicate the depth of sleep is defined.
P-3: Functions to obtain the mean incidence ratio of each sleep stage and the standard deviation are determined for healthy subjects of each age group.
P-4: An algorithm to classify similar sleep stages to those used in the R–K method is proposed.
P-5: A method to realize the aforementioned algorithm without having to wear any sensor device on a human's body.

III. Proposed Methods

A. Index Characterizing REM Sleep

With regard to the issue P-1, a REM sleep index is defined using the heartbeat signal. Table I shows the characteristics of REM sleep described in [2] and [18].

The R–K method, in determining the REM sleep stage, focuses on brain waves, eye movement, and the EMG of jaw muscle, as shown in characteristics No. 1–No. 4 in Table I. This paper focuses on the fact that the heartbeat becomes less rhythmical during REM sleep (characteristic No. 5 in Table I).

The discrete time for every 1 min is defined as k, and the value changes from $k = 1, 2, \ldots$, to TIB. TIB represents the

TABLE I
CHARACTERISTICS OF REM SLEEP

No.	Characteristics of REM sleep
1	Brainwaves similar to those shown in Non-REM 1 and Wake stages are found
2	The incidence ratios of delta wave and spindle wave decrease
3	The tension of anti-gravity muscles completely disappears
4	Rapid eye movement appears
5	Heartbeat and respirations become more frequent and less rhythmical, and the blood pressure becomes high
6	With regard to adults, REM sleep occurs once every 90 to 100 minutes on average
7	Body movement is concentrated before and after REM sleep

TABLE II
CHARACTERISTICS OF NON-REM SLEEP

No.	Characteristics of Non-REM sleep
1	The deeper the person sleeps, the more frequent the incidence ratio of delta waves
2	In the sleep stage of Non-REM2, spindle waves are recognized
3	When sleep deepens from the Wake stage, body movements become smaller and less frequent
4	The deeper the sleep, the less frequent the heart rate
5	Non-REM1 occasionally is found after Non-REM3, Non-REM4, or REM sleep stages with large body movement

total measurement time (in minutes) with a subject lying on the bed. Let H_k^{former} be the heart rate of the former 30 s of the 1 min of discrete time k. Similarly, let H_k^{latter} be the heart rate of the latter 30 s of the discrete time k. The change of heart rate between the former and latter halves of the 1-min discrete time k is thus obtained from $|H_k^{\text{former}} - H_k^{\text{latter}}|$. The same procedures are performed for each of $k = 1, 2, \ldots, TIB$, and the index $R(k)$ to show the REM sleep stages as in (1) is obtained through the moving average for the range from $k - q$ to $k + q$

$$R(k) = \frac{1}{2q+1} \sum_{i=-q}^{q} \left| H_{k+i}^{\text{former}} - H_{k+i}^{\text{latter}} \right|. \tag{1}$$

The values of the index $R(k)$ become large during REM sleep due to the aforementioned characteristic No. 5 of REM sleep in Table I.

B. Index Characterizing the Wake and Non-REM Sleep

With regard to the issue P-2, a sleep depth index is defined using the heartbeat and body-movement signals. Table II shows the characteristics of Wake and Non-REM sleeps described in [2] and [18].

The sleep depth index is defined based on the fact "When sleep deepens, body movement becomes smaller and less frequent." as shown in characteristic No. 3 in Table II.

Let A_k^{body} and A_k^{heart} be the mean amplitudes of the body-movement and the heartbeat signals, respectively, at the discrete time k. The value of A_k^{body} becomes large when the sleep is shallow, as the body movement is frequent. When the sleep is deep, on the other hand, the value of A_k^{body} becomes rather small. The amplitudes of the body-movement and heartbeat signals vary with differences in the subjects. In order to standardize these deviations, A_k^{body} is divided by $A_k^{\text{heart}} + A_k^{\text{body}}$. A_k^{body} largely fluctuates when body movement is detected and when not detected at all. A_k^{body} subtly fluctuates when a few body movements are detected. In order to reduce the large fluctuations and to magnify the subtle ones, the logarithm of $A_k^{\text{body}}/(A_k^{\text{heart}} + A_k^{\text{body}})$ is calculated, and the sleep depth index $D(k)$ becomes

$$D(k) = \log_2 \left(\frac{A_k^{\text{body}}}{A_k^{\text{heart}} + A_k^{\text{body}}} \right). \tag{2}$$

The value of the index $D(k)$ becomes small when the sleep is deep, and the shallower the sleep, the larger the value.

C. Incidence Ratios of the Sleep Stages for Subjects of Each Age Group

With regard to the issue P-3, the functions, which calculate the mean incidence ratio of each sleep stage and its standard deviation to the input data of a subject's age, are determined.

We determined these functions based on the approximate values of the fourth-order curve against the incidence ratio of each sleep stage for 306 subjects aged between 3 and 96 years old. These 306 subjects' data were quoted from [19] to [22].

Let a be age. The incidence ratios of each sleep stage, namely, $r_{\text{Wake}}(a)$, $r_{\text{REM}}(a)$, $r_{\text{NR1}}(a)$, $r_{\text{NR2}}(a)$, $r_{\text{NR3}}(a)$, and $r_{\text{NR4}}(a)$, are obtained from (3), (5), (7), (9), (10), and (11), respectively, and the standard deviations of each sleep stage, namely, $\delta r_{\text{Wake}}(a)$, $\delta r_{\text{REM}}(a)$, $\delta r_{\text{NR1}}(a)$, $\delta r_{\text{NR2}}(a)$, $\delta r_{\text{NR3}}(a)$, and $\delta r_{\text{NR4}}(a)$, are obtained from (4), (6), (8), (10), (12), and (14), respectively

(Wake)

$$r_{\text{Wake}}(a) = -3.07 \times 10^{-6} a^4 + 6.02 \times 10^{-4} a^3 - 3.23 \times 10^{-2} a^2 + 5.99 \times 10^{-1} a - 1.70 \times 10^{0}$$
$$R^2 = 0.93 \tag{3}$$

$$\delta r_{\text{Wake}}(a) = -1.26 \times 10^{-6} a^4 + 2.45 \times 10^{-4} a^3 - 1.24 \times 10^{-2} a^2 + 2.41 \times 10^{-1} a + 1.41 \times 10^{-2}$$
$$R^2 = 0.72 \tag{4}$$

(REM)

$$r_{\text{REM}}(a) = 3.36 \times 10^{-6} a^4 - 6.89 \times 10^{-4} a^3 + 4.55 \times 10^{-2} a^2 - 1.19 \times 10^{0} a + 3.50 \times 10$$
$$R^2 = 0.88 \tag{5}$$

$$\delta r_{\mathrm{REM}}(a) = 1.14 \times 10^{-6}a^4 - 1.60 \times 10^{-4}a^3 + 6.63 \times 10^{-3}a^2 - 6.02 \times 10^{-2}a + 3.49 \times 10^{0}$$

$$R^2 = 0.52 \tag{6}$$

(Non-REM1)

$$r_{\mathrm{NR1}}(a) = -4.20 \times 10^{-7}a^4 + 1.17 \times 10^{-4}a^3 - 8.61 \times 10^{-3}a^2 + 3.12 \times 10^{-1}a + 5.82 \times 10^{-1}$$

$$R^2 = 0.82 \tag{7}$$

$$\delta r_{\mathrm{NR1}}(a) = 1.02 \times 10^{-6}a^4 - 1.58 \times 10^{-4}a^3 + 7.83 \times 10^{-3}a^2 - 8.71 \times 10^{-2}a + 1.52 \times 10^{0}$$

$$R^2 = 0.65 \tag{8}$$

(Non-REM2)

$$r_{\mathrm{NR2}}(a) = 2.82 \times 10^{-6}a^4 - 6.00 \times 10^{-4}a^3 + 3.46 \times 10^{-2}a^2 - 4.06 \times 10^{-1}a + 4.77 \times 10$$

$$R^2 = 0.65 \tag{9}$$

$$\delta r_{\mathrm{NR2}}(a) = 1.66 \times 10^{-6}a^4 - 2.49 \times 10^{-4}a^3 + 1.14 \times 10^{-2}a^2 - 7.75 \times 10^{-2}a + 4.78 \times 10^{0}$$

$$R^2 = 0.56 \tag{10}$$

(Non-REM3)

$$r_{\mathrm{NR3}}(a) = 4.37 \times 10^{-8}a^4 + 2.15 \times 10^{-5}a^3 - 5.92 \times 10^{-3}a^2 + 3.27 \times 10^{-1}a + 1.57 \times 10^{0}$$

$$R^2 = 0.51 \tag{11}$$

$$\delta r_{\mathrm{NR3}}(a) = -4.94 \times 10^{-7}a^4 + 8.00 \times 10^{-5}a^3 - 4.69 \times 10^{-3}a^2 + 1.54 \times 10^{-1}a + 4.77 \times 10^{-1}$$

$$R^2 = 0.56 \tag{12}$$

(Non-REM4)

$$r_{\mathrm{NR4}}(a) = -2.74 \times 10^{-6}a^4 + 5.49 \times 10^{-4}a^3 - 3.33 \times 10^{-2}a^2 + 3.58 \times 10^{-1}a + 1.68 \times 10$$

$$R^2 = 0.96 \tag{13}$$

$$\delta r_{\mathrm{NR4}}(a) = 1.66 \times 10^{-6}a^4 - 2.60 \times 10^{-4}a^3 + 1.07 \times 10^{-2}a^2 - 5.30 \times 10^{-2}a + 3.36 \times 10^{0}$$

$$R^2 = 0.50. \tag{14}$$

In these equations, R^2 indicates the determination coefficient. The domain of a is set between 3 and 92, which is the age range of the 306 subjects whose data were used to make these functions. The reason for using the fourth order in (3)–(14) is because using the fifth or larger order would hardly affect the determination coefficient. Fig. 1 shows the mean incidence ratios of each sleep stage and the range of incidence ratios by standard deviation which are shown by the gray area obtained from (3)–(14). As shown in Fig. 2, $r_{\mathrm{Wake}}(a) + r_{\mathrm{REM}}(a) + r_{\mathrm{NR1}}(a) + r_{\mathrm{NR2}}(a) + r_{\mathrm{NR3}}(a) + r_{\mathrm{NR4}}(a)$ equals 100%. The older the subjects, the more frequent the incidence ratio of the Wake stage and the less frequent the ratio of deeper sleep stages.

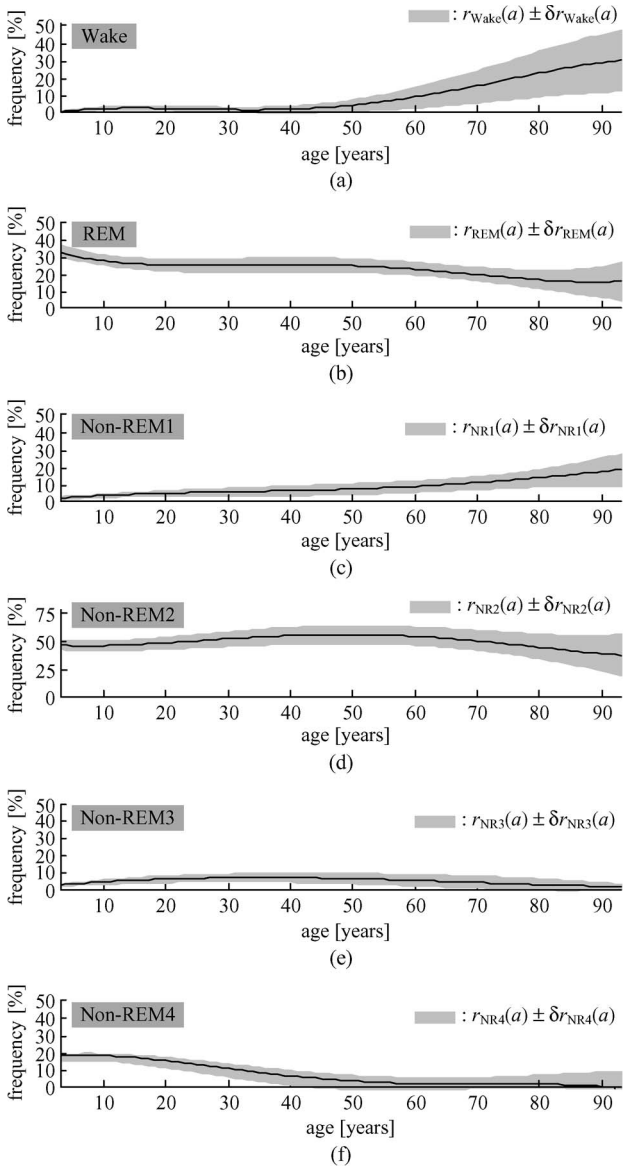

Fig. 1. Mean incidence ratio and range of incidence ratio by standard deviation of each sleep stage for each age group. (a) Wake, (b) REM, (c) Non-REM1, (d) Non-REM2, (e) Non-REM3, (f) Non-REM4.

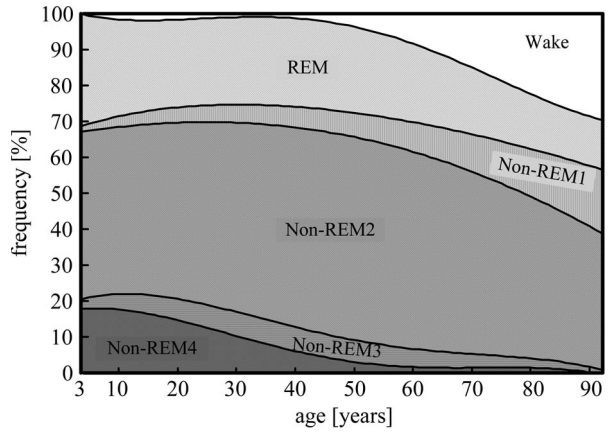

Fig. 2. Mean incidence ratio and standard deviation of each sleep stage for each age group.

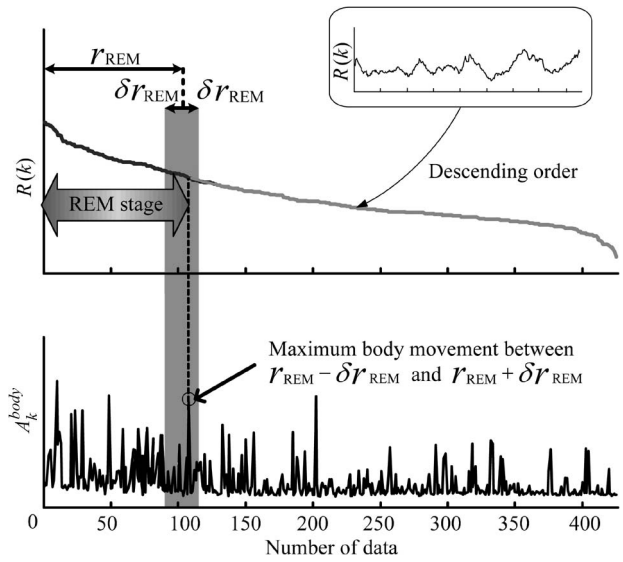

Fig. 3. Classification of REM stage.

D. Sleep-Stage Classification

With regard to the issue P-4, the REM sleep periods are estimated based on the REM sleep index of $R(k)$ and (5) and (6). The ages of the subjects are input into a in (5) and (6) to obtain $r_{\mathrm{REM}}(a)$ and $\delta r_{\mathrm{REM}}(a)$, where the incidence ratio of REM sleep is assumed to be within $r_{\mathrm{REM}}(a) \pm \delta r_{\mathrm{REM}}(a)$. As shown in Fig. 3, the values of REM sleep index of $R(k)$ are juxtaposed in descending order, and the period whose smallest $R(k)$ value corresponds to the largest body movement of A_k^{body} is classified to REM sleep. This is based on characteristic No. 7 of REM sleep in Table I.

Next, based on the $D(k)$ and (3), (4), and (7)–(14), the periods for Wake and Non-REM1 through Non-REM4 sleep stages are classified. The value of sleep depth index $D(k)$, except for those classified to REM sleep, are juxtaposed in descending order as shown in Fig. 4. As with the REM sleep case, the ages of the subjects are input into (3), (4), and (7)–(14) to obtain the incidence ratio of each sleep stage: Wake, Non-REM1, Non-REM2, Non-REM3, and Non-REM4. As shown in Figs. 1 and 2, even if the subjects' ages are the same, their incidence ratios of each sleep stage appear in the range of mean $\pm$ standard deviation. Therefore, the incidence ratio of each stage is assumed to be within the ranges shown as follows:

$$\begin{aligned}
&\text{Wake}: && [r_{\mathrm{Wake}}(a) - \delta r_{\mathrm{NR1}}(a), r_{\mathrm{Wake}}(a) + \delta r_{\mathrm{Wake}}(a)]\\
&\text{Non-REM1}: && [r_{\mathrm{NR1}}(a) - \delta r_{\mathrm{NR2}}(a), r_{\mathrm{NR1}}(a) + \delta r_{\mathrm{NR1}}(a)]\\
&\text{Non-REM2}: && [r_{\mathrm{NR2}}(a) - \delta r_{\mathrm{NR3}}(a), r_{\mathrm{NR2}}(a) + \delta r_{\mathrm{NR2}}(a)]\\
&\text{Non-REM3}: && [r_{\mathrm{NR3}}(a) - \delta r_{\mathrm{NR4}}(a), r_{\mathrm{NR3}}(a) + \delta r_{\mathrm{NR3}}(a)]\\
&\text{Non-REM4}: && [r_{\mathrm{NR4}}(a) - \delta r_{\mathrm{NR3}}(a), r_{\mathrm{NR4}}(a) + \delta r_{\mathrm{NR4}}(a)]\,.
\end{aligned}$$

The incidence ratios of Wake and Non-REM1, as with the REM sleep, apply the values whose corresponding body movements A_k^{body} are the largest within the range. With regard to the incidence ratios of Non-REM2 through Non-REM4, the values where the slope of $D(k)$ is the largest within the ranges are applied, respectively. Based on these incidence ratios, periods for Wake and Non-REM1 through Non-REM4 sleep stages are classified.

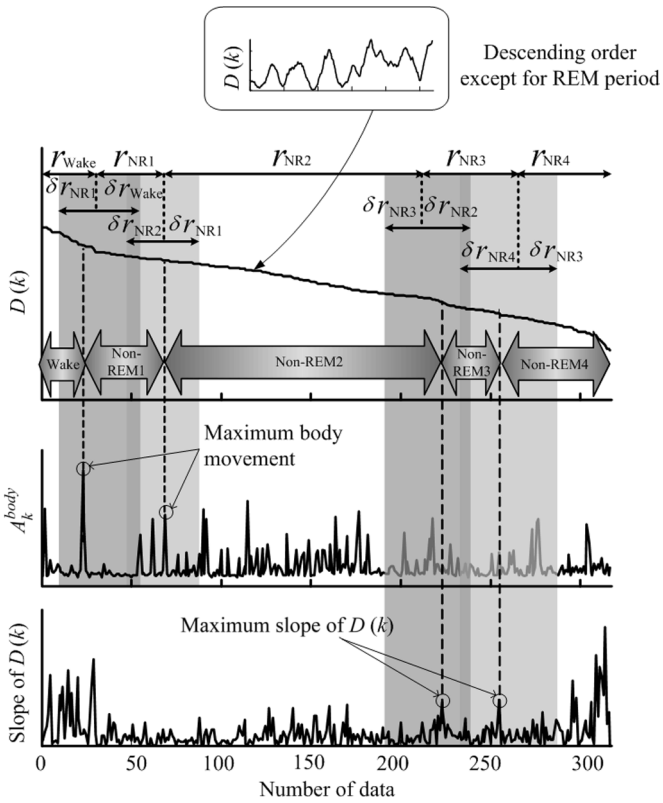

Fig. 4. Classification of Wake and Non-REM stages.

After the classifications, the values are rejuxtaposed chronologically to obtain the sleep stages equivalent to those used for the R–K method.

E. Pneumatic Method for Unconstrained Biosensing Method to Measure Heartbeat and Body Movement

With regard to the issue P-5, we have proposed a pneumatic method which can measure biosignals without having to wear any sensor device on a human's body. Fig. 5 shows the mechanism of our proposed pneumatic method. A vinyl-coated air mattress of about 5 mm in thickness is placed under an ordinary bed cushion (or futon mattress). The inner pressure of the air mattress is equivalent to atmospheric pressure. When a person lies on the bed cushion, heartbeat, respiration, and body movement (such as rolling over) are conveyed to the air inside the air mattress through the bed cushion. The change in air pressure is measured with a highly sensitive pressure sensor (Primo Co. Ltd.). The pressure sensor is capable of measuring pressure changes between 0.002 and 20 Pa, and its sensitivity is constant between the frequencies of 0.1 and 3.0 kHz [16]. Because the signals measured by the pressure sensor contain heartbeat, respiration, and body-movement components, the signals are input into a biosignal filter circuit, where they go through a bandpass filter to extract heartbeat components. The frequency ranges of heartbeat and respiration signals are about 0.8–1.5 Hz and 0.2–0.8 Hz, respectively. When the frequency of heartbeat is low and that of respiration is high, the frequency of

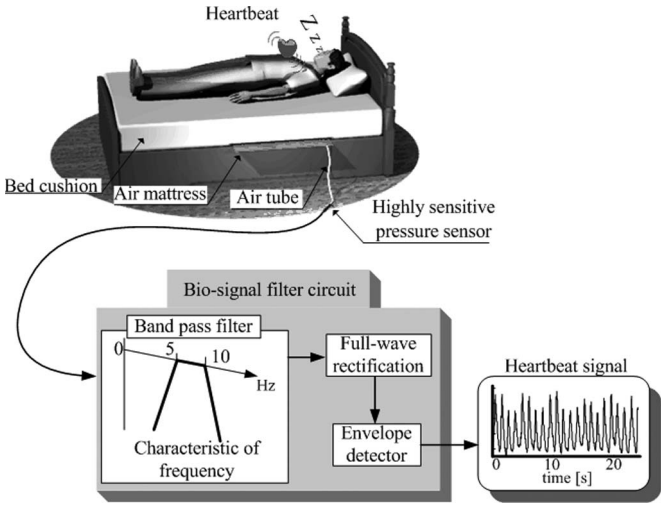

Fig. 5. Unconstrained and noninvasive biomeasurement by the pneumatic method.

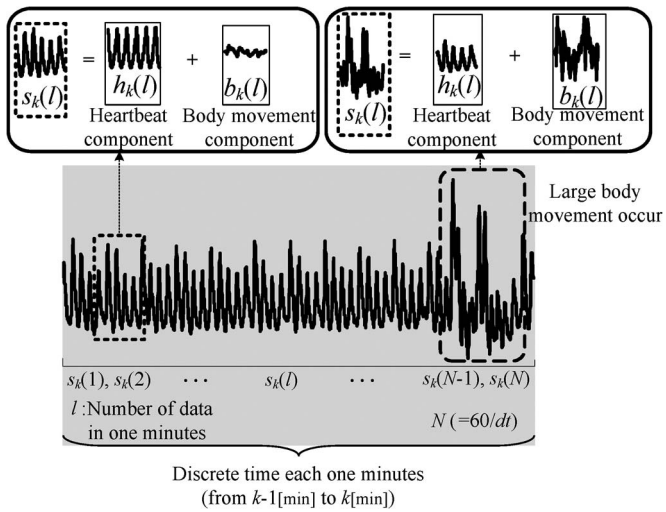

Fig. 6. Biosignal measured by pneumatic method.

the heartbeat and respiration signals may overlap, which makes it difficult to distinguish the signals for filtering. In order to distinguish the heartbeat and respiration signals, we extracted harmonic components of the heartbeat signals because respiration signals do not include strong harmonic components compared with heartbeat signals. Therefore, we chose 5–10 Hz as the frequency range of the bandpass filter. The signals then undergo full-wave rectification and envelope processing and are output from the circuit.

Furthermore, body-movement signals contain many low-frequency components similar to heartbeat signals. However, even if heartbeat signals are extracted in the range of 5–10 Hz, they are strongly affected by body-movement signals because the amplitude of the body-movement signals is significantly larger than that of the heartbeat and respiration signals. Hence, regarding distinguishing the heartbeat and body-movement signals, we need to apply further signal processing to the output signals from the biosignal filter circuit as described in the following sections.

F. Signal-Processing Flow to Calculate Heart Rate

The sampling signals that are output from the biosignal filter circuit are taken at the interval of $dt = 0.01$ s and are saved as time-series data as shown in Fig. 6. The discrete time at the interval of dt within each minute out of the discrete time k is defined as l, and the value changes from $l = 1, 2, \ldots,$ to $N(= 60/dt)$. When the heartbeat component and the body-movement component at the discrete times of k and l are defined as $h_k(l)$ and $b_k(l)$, respectively, the output from the biosignal filter circuit $s_k(l)$ is obtained from the linear combination of the heartbeat component and the body-movement component as follows:

$$s_k(l) = h_k(l) + b_k(l). \tag{15}$$

If the heartbeat component $h_k(l)$ can be separated from $s_k(l)$ in (15), it will be possible to accurately estimate the heart rate. We have separated the heartbeat and body-movement components from the base frequencies, their harmonic components, and other components, by applying fast Fourier transform (FFT) to the output signals from the sensor [17]. However, body movements such as rolling over contain many low-frequency components close to the heart rate, and the heart rate obtained from the FFT peak spectrum occasionally contained errors. In this paper, a method using comb filters that effectively uses the heartbeat and its harmonic components to accurately separate the heartbeat and body movement is proposed.

If the delay time of the comb filters is defined as T, T/dt in terms of a discrete time is obtained. When the feedback gain of the comb filter is defined as $g_h (0 \leq g_h \leq 1)$, the heartbeat component $\hat{h}_k(l)$ at the discrete times of k and l is shown as output data from the comb filter as given by the following equation:

$$\hat{h}_k(l) = s_k(l) + s_k\left(l - \frac{T}{dt}\right) + g_h \cdot \hat{h}_k\left(l - \frac{T}{dt}\right). \tag{16}$$

The frequency characteristics of the comb filter in (16) are shown in Fig. 7. The filters of (16), as shown in Fig. 7, peak at the direct-current component and at the frequencies that correspond to integer multiples of $1/T$. The sharpness of the peaks of the frequency characteristic shown in Fig. 7 varies with the feedback gain g_h: The closer the feedback gain g_h is to one, the sharper the wave shape. When T in (16) is close to the actual heartbeat cycles, the filters in (16) amplify the amplitude of the heartbeat component. Fig. 8 shows the juxtaposition of 78 comb filters for (16) with the delay times T of 0.66, 0.67, 0.68, ..., 1.43 s. The delay time of the first comb filter is $T = 0.66$ s, and it resonates with the heartbeat cycle of 90 times/min as the frequency peaks at integer multiples of 1.51 Hz. Similarly, the 78th comb filter, with the delay time of $T = 1.43$ s, has its peak frequencies at the integer multiples of 0.7 Hz; thus, it resonates with the heartbeat of 42 times/min. The delay-time resolution of these comb filters is $60dt/T^2$ for a minute of heartbeat: 1.35 times/min for the heartbeat of 90 times/min and 0.29 times/min for that of 42 times/min. These 78 comb filters therefore encompass the heartbeat between 42 and 90 times/min with the mean resolution of 0.82 times/min.

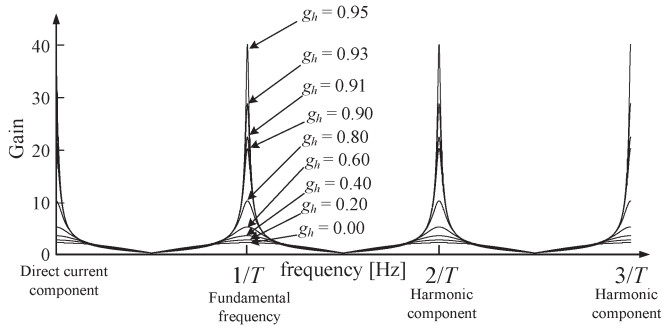

Fig. 7. Frequency characteristics of comb filter in (16).

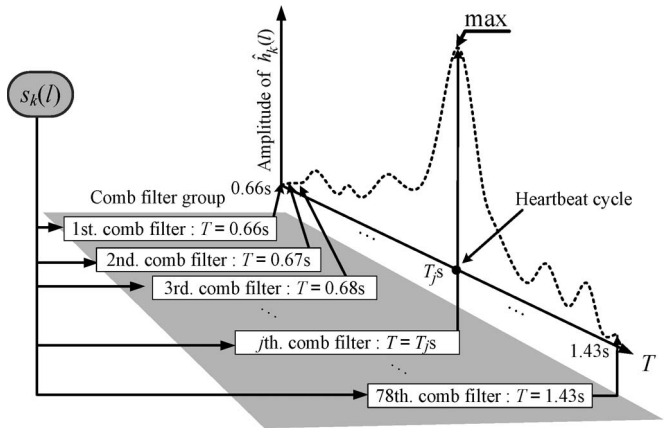

Fig. 8. Heartbeat-cycle estimation by comb-filter group.

The data for the former 30 s of the 1 min of the discrete time k, namely, $s_k(1), s_k(2), s_k(3), \ldots, s_k(N/2)$, are input into these comb filters, and their output data $\hat{h}_k(l)$ obtained from these comb filters are compared for their amplitudes. The delay time T of the comb filter with the largest amplitude for $\hat{h}_k(l)$ is estimated to be the heartbeat cycle T_k^{former} in the former 30 s. Similarly, the delay time where the amplitude $\hat{h}_k(l)$ becomes the largest against the input data among the latter 30 s of the discrete time k, namely, $s_k(N/2+1), s_k(N/2+2), s_k(N/2+3), \ldots, s_k(N)$, is determined as T_k^{latter}. Therefore, the heart rates of the former 30 s H_k^{former} and latter 30 s H_k^{latter} in (1) are $H_k^{\text{former}} = 60/T_k^{\text{former}}$ and $H_k^{\text{latter}} = 60/T_k^{\text{latter}}$, respectively.

G. Signal-Processing Flow to Calculate the Amplitude of the Body Movement

To calculate the A_k^{body} in (2), we consider a different comb filter from (16). When the feedback gain of the comb filter is defined as g_b $(0 \le g_b \le 1)$, the body-movement component $\hat{b}_k(l)$ at the discrete times of k and l is shown as output data from the comb filter as given by the following equation:

$$\hat{b}_k(l) = s_k(l) - s_k\left(l - \frac{T}{dt}\right) + g_b \cdot \hat{b}_k\left(l - \frac{T}{dt}\right). \qquad (17)$$

The frequency characteristics of the comb filter in (17) are shown in Fig. 9. The gains for the filter of (17), as shown in Fig. 9, become zero at the same frequencies where the gains peaked in Fig. 7.

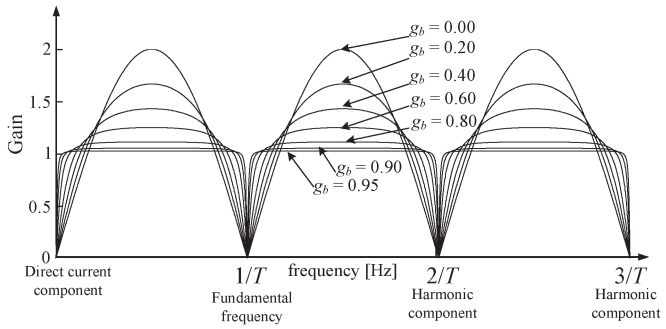

Fig. 9. Frequency characteristics of the comb filter in (17).

When T in (16) is close to the actual heartbeat cycles, the filter in (16) amplifies the amplitude of the heartbeat component, whereas the filter in (17) attenuates the heartbeat component and amplifies the body-movement component. The output data $\hat{b}_k(l)$ of (17) at the delay time T, which is close to the heartbeat cycle, indicate attenuation in the heartbeat component and amplification in the body-movement component. The mean amplitude of the output from (17) with the same T used for estimating the heart rate at the discrete time k is determined as A_k^{body}.

Then, $A_k^{\text{heart}} + A_k^{\text{body}}$ in (2) is determined as the mean amplitude of the $s_k(l)$ because of the linearity shown in (15).

IV. Verification Experiment

A. Subjects and Experimental Environment

The experiment was carried out on ten healthy adult male subjects (A–J) with the mean age of 22.2 years old. After obtaining informed consent from each of them, their sleeps were measured for 20 nights. The measurement environment was as shown in Fig. 10. Heartbeat and body movement were measured using the pneumatic method. The brain waves and eye movement were also measured simultaneously using a polygraph (SANYOFIT2500NEC San-ei) to be compared with the heartbeat and sleep stages.

B. Verification of the Validity of REM Sleep Index

With regard to the verification of the issue P-1, Fig. 11 shows the $R(k)$ of subject F's second night, the incidence ratios of delta wave and spindle wave among the brain waves, and the incidence ratio of REM, all of which were measured with a polygraph. The order of the moving average of $R(k)$ in (1) was set to $q = 10$. In addition, the gain g_h of the comb filters shown in Fig. 8 was set to $g_h = 0.95$. When the $R(k)$ value is large, the fluctuation of heart rate is also large. This, in light of characteristic No. 5 of REM sleep in Table I, shows the high possibility of the appearance of REM sleep. During the periods shown in gray in Fig. 11, the incidence ratios of delta wave and spindle wave are low, and the appearance of REM is rather frequent, indicating characteristics No. 2 and No. 4 of REM sleep. During their corresponding periods, the values of the REM sleep index $R(k)$ are rather large. The periods when the $R(k)$ takes large values appear roughly once every 100 min, as indicated in characteristic No. 6 of REM sleep. This shows that

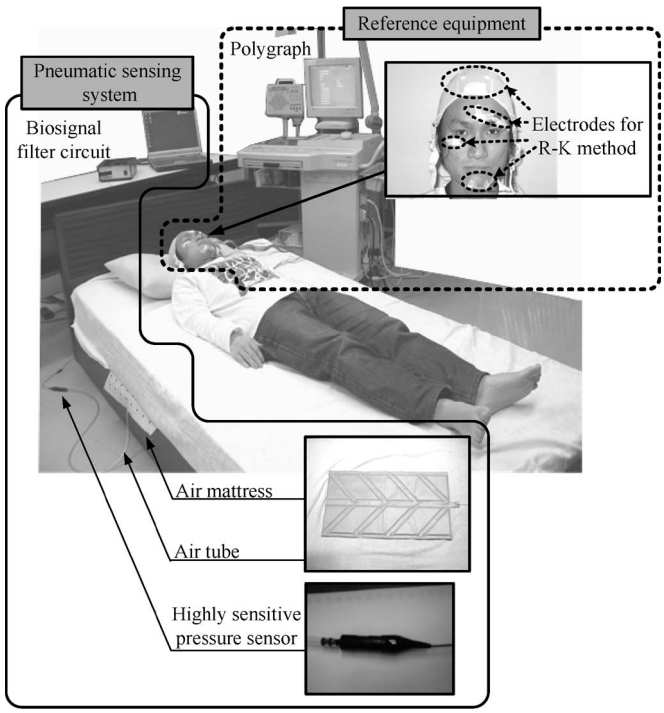

Fig. 10. Measurement system.

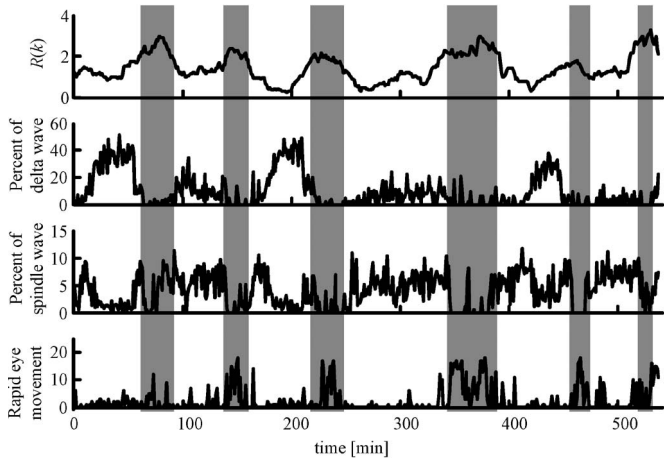

Fig. 11. $R(k)$, percent of delta wave, percent of spindle wave, and number of REMs each minute.

the concurrent appearances of the REM sleep characteristics No. 2, No. 4, and No. 5 during a REM sleep enable the appearance of REM sleep to be estimated with the index $R(k)$.

C. Verification of Validity of Sleep Depth Index

With regard to the verification of the issue P-2, the function g_b in (17) is set to $g_b = 0.8$. Fig. 12 shows the $D(k)$ and delta wave of F-2. The periods shown in gray in the figure show high incidence ratios of delta wave, and this indicates a deep-sleep stage as indicated by characteristic No. 1 of Non-REM sleep in Table II. During these periods, the value of $D(k)$ becomes small. This shows that the concurrent appearances of the Non-REM sleep characteristics No. 1 and No. 3 enabled the sleep depth to be estimated using the sleep depth index $D(k)$.

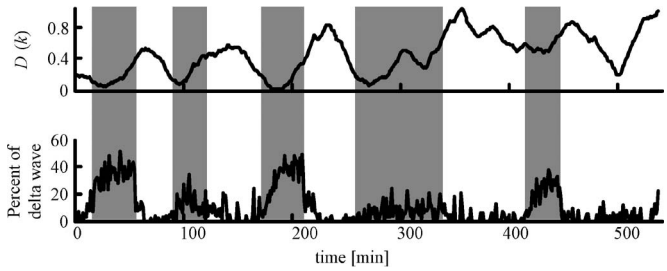

Fig. 12. $D(k)$ and percent of delta wave each minute.

D. Classification of Sleep Stages

With regard to the verification of the issue P-4, sleep stages are determined using the algorithm described in Section III-D, and the stages are compared with those determined by the R–K method. Fig. 13 shows the classified six sleep stages based on $R(k)$ and $D(k)$ and the classified sleep stages based on the R–K method.

A comparison between the sleep stages classified with $R(k)$ and $D(k)$ and the sleep stages classified with the R–K method indicates they have generally similar wave shapes such as: the places where the 100-min cycle of REM sleep appears as shown in characteristic No. 6 in Table II and in the sleep stages that become shallower toward dawn. However, with regard to the periods around 100 min and around 280 min, the proposed method determined these as Non-REM4, whereas the R–K method judged them as Non-REM2. The period around 470 min was determined as Wake by the proposed method but as REM sleep by the R–K method. The agreement ratios of the classification results of each method against $TIB[number\ of\ agreements/TIB \times 100(\%)]$ and the kappa statistics were used for the comparison. The agreement ratio and the kappa statistics (see the Appendix), for a one-night sleep of $TIB = 537$ min with the sleep stages classified into six as shown in Fig. 13, were 52.1% and 0.25, respectively. Table III shows TIB, the agreement ratios, and the kappa statistics corresponding to the sleep stages classified into six stages of all subjects and also shows their mean values and standard deviations. Fig. 14 shows the sleep stages classified into five stages (Non-REM3 and Non-REM4 are classified as the same stage as a deep-sleep stage [22]) by each method. The agreement ratio and the kappa statistics were 58.7% and 0.38, respectively. Table IV shows the agreement ratios and the kappa statistics corresponding to the sleep stages classified into five stages of all subjects and also shows their mean values and standard deviations. Moreover, Fig. 15 shows the sleep stages classified into three stages (Non-REM1–Non-REM4 are classified as the same stage as a Non-REM sleep stage) by each method. The agreement ratio and the kappa statistics were 79.5% and 0.46, respectively. Table V shows the agreement ratios and the kappa statistics corresponding to the sleep stages classified into three stages of all subjects and also shows their mean values and standard deviations.

V. Discussion

With regard to each sleep-stage classification, the agreement ratios and the kappa statistics of the other subjects in

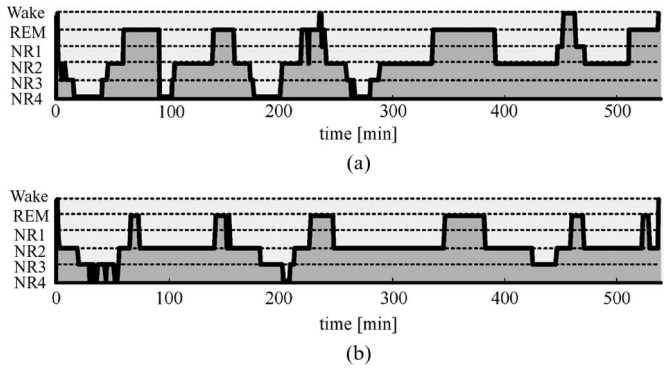

Fig. 13. Classification of sleep stages into Wake, REM, Non-REM1, Non-REM2, Non-REM3, and Non-REM4. (a) Pneumatic method, (b) R–K method.

TABLE III
SLEEP-STAGE AGREEMENT AND KAPPA STATISTICS BETWEEN THE PROPOSAL METHOD AND THE R–K METHOD (WAKE, REM, NON-REM1, NON-REM2, NON-REM3, AND NON-REM4)

Subject	Trial	*TIB* [min]	Wake, REM, Non-REM1,2,3,4	
			Agreement [%]	Kappa
A	1st	377	53.3	0.33
	2nd	247	41.3	0.27
B	1st	404	54.7	0.35
	2nd	387	54.5	0.37
C	1st	545	51.9	0.23
	2nd	434	55.5	0.29
	3rd	402	64.7	0.37
	4th.	509	50.5	0.32
D	1st	441	52.2	0.22
E	1st.	466	49.4	0.30
	2nd	425	57.2	0.33
F	1st	437	54.2	0.29
	2nd	537	52.1	0.25
	3rd	358	48.3	0.23
G	1st	464	46.6	0.36
H	1st	496	48.8	0.27
I	1st	483	50.7	0.29
	2nd	448	50.0	0.20
J	1st	551	49.4	0.20
	2nd	569	47.5	0.32
MEAN		449	51.6	0.29
S.D.		75	4.6	0.05

Tables III–V, like the subject for F's second night increase as the number of the classification decreases from six to three. In the previous works [15] and [17], we also evaluated the sleep-stage agreement. The average agreement ratios for the six stages in the previous works were 42.8% and 36.4%, whereas by the proposed method, the agreement is 51.6%, as shown in Table III. Thus, the proposed algorithm improved the precision by about 10%–15%. The mean value of its corresponding kappa statistics was 0.29 including the errors due to coincidences. For the sleep stages classified into five, the mean agreement ratio increased by 4.6%–56.2%, and the ratio was 77.5% for the classification into three stages. This is because the disagreement ratio is larger among Non-REM1, Non-REM2, and Non-REM3/Non-REM4 than between Non-REM3 and Non-REM4. The average of the kappa statistics was 0.39 for the sleeps classified into five and 0.48 for those classified into three, and the general sleep patterns and the rhythms of REM and Non-REM sleeps can thus be identified.

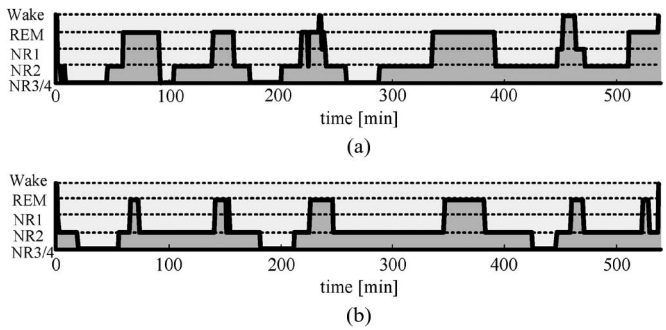

Fig. 14. Classification of sleep stages into Wake, REM, Non-REM1, Non-REM2, and Non-REM3/Non-REM4. (a) Pneumatic method, (b) R–K method.

TABLE IV
SLEEP-STAGE AGREEMENT AND KAPPA STATISTICS BETWEEN THE PROPOSAL METHOD AND THE R–K METHOD (WAKE, REM, NON-REM1, NON-REM2, AND NON-REM3/NON-REM4)

Subject	Trial	Wake, REM, Non-REM1,2,3/4	
		Agreement [%]	Kappa
A	1st	64.2	0.41
	2nd	47.0	0.34
B	1st	57.9	0.46
	2nd	57.9	0.47
C	1st	60.2	0.37
	2nd	61.8	0.44
	3rd	66.9	0.39
	4th.	54.4	0.37
D	1st	37.6	0.34
E	1st.	53.7	0.39
	2nd	63.8	0.51
F	1st	60.4	0.41
	2nd	58.7	0.38
	3rd	54.8	0.39
G	1st	52.2	0.39
H	1st	54.2	0.37
I	1st	54.7	0.38
	2nd	56.5	0.28
J	1st	54.8	0.32
	2nd	53.4	0.35
MEAN		56.2	0.39
S.D.		6.3	0.05

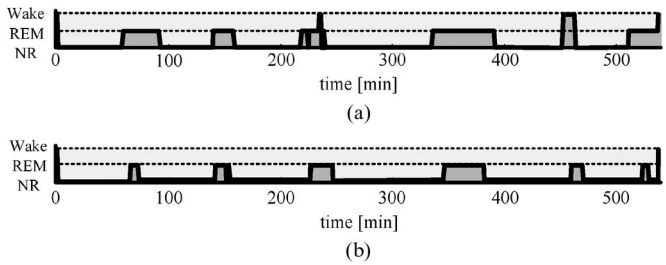

Fig. 15. Classification of sleep stages into Wake, REM, and Non-REM. (a) Pneumatic method, (b) R–K method.

The proposed algorithm allows us to monitor and improve the quality of daily sleep at home. High-quality sleep is important for good health and preventing sleep-related diseases such as narcolepsy and insomnia.

TABLE V
SLEEP-STAGE AGREEMENT AND KAPPA STATISTICS BETWEEN THE PROPOSAL METHOD AND THE R–K METHOD (WAKE, REM, AND NON-REM)

Subject	Trial	Wake, REM, Non-REM	
		Agreement [%]	Kappa
A	1st	80.9	0.56
	2nd	77.3	0.40
B	1st	80.0	0.51
	2nd	87.1	0.60
C	1st	74.9	0.42
	2nd	81.8	0.48
	3rd	85.1	0.57
	4th.	80.8	0.45
D	1st	59.9	0.37
E	1st.	75.1	0.46
	2nd	87.5	0.67
F	1st	77.6	0.47
	2nd	79.5	0.46
	3rd	71.5	0.49
G	1st	77.6	0.48
H	1st	74.6	0.42
I	1st	70.4	0.44
	2nd	78.6	0.42
J	1st	78.0	0.43
	2nd	71.0	0.51
MEAN		77.5	0.48
S.D.		6.2	0.07

VI. CONCLUSION

In this paper, the REM sleep index $R(k)$ and the sleep depth index $D(k)$ have been determined, and the relationships of these indices with the periods when the delta wave, spindle wave, and REM occur have been examined. When REM was frequent, and the delta wave and spindle wave were not frequently observed, the $R(k)$ value was large, indicating a high possibility of REM sleep incidence. The $D(k)$ value, on the other hand, is a small value when the incidence of delta wave is frequent, and the value changes from large to small corresponding to the change in sleep depth from Wake to Non-REM1, Non-REM2, Non-REM3, and Non-REM4. In order to estimate the sleep stages based on these two indices, the coefficients for the fourth-order curve to calculate the mean incidence ratio and the standard deviation of each sleep stage were determined. It was shown that using these two indices, the incidence ratio of each sleep stage, and its corresponding standard deviation, improved the accuracy of estimating the sleep stage compared with the conventional method.

The proposed algorithm depends on the measurements of the heartbeat and body movement by the pneumatic method presented in [16]. The novelty of the algorithm in comparison with that in [15] which also depends on the pneumatic method is the use of the two indices $D(k)$ and $R(k)$ and the information on sleep-stage characteristics determined by age. The proposed algorithm improves the precision by about 10% in comparison with the result in [15].

One of our ultimate objectives is to apply our system to elderly people for improving the quality of their sleep. As a preliminary step, in this study, we carried out experiments using young subjects to verify the accuracy of the proposed algorithm. We now intend to conduct verification experiments using subjects with a wider range of age.

TABLE VI
KAPPA STATISTICS

		Score A		
		a	b	c
Score B	a	$f_{1,1}$	$f_{1,2}$	$f_{1,3}$
	b	$f_{2,1}$	$f_{2,2}$	$f_{2,3}$
	c	$f_{3,1}$	$f_{3,2}$	$f_{3,3}$

APPENDIX
KAPPA STATISTICS

The kappa statistic is an index that shows the degree of coincidence of judgments among plural scorers. As an example, here, we consider two scorers A and B for three items a, b, and c as listed in Table VI.

Table VI shows judgment frequency $f_{i,j}$ for three items a, b, and c by two scorers A and B. Let

$$P_o = \frac{\sum_{i=1}^{3} f_{i,i}}{\sum_{i=1}^{3}\sum_{j=1}^{3} f_{i,j}}$$

and

$$P_e = \frac{\sum_{i=1}^{3} f_{1,i} \sum_{j=1}^{3} f_{j,1} + \sum_{i=1}^{3} f_{2,i} \sum_{j=1}^{3} f_{j,2} + \sum_{i=1}^{3} f_{1,3} \sum_{j=1}^{3} f_{j,3}}{\sum_{i=1}^{3}\sum_{j=1}^{3} f_{i,j}}.$$

Then, the kappa statistic κ is defined as $\kappa = (P_o - P_e)/(1 - P_e)$.

REFERENCES

[1] R. Kawahara, H. Maeda, and S. Yoshioka, "Sleep disorder as a modern disease," Japan Rev., Tokyo, Japan, 2000.

[2] S. Chiba and K. Homma, *The Clinic of Circadian Sleep Disorder*. Tokyo, Japan: Shinko Med. Publ., 2003.

[3] Japan General Research Institutes, Report on New Industrial Generation on Health Care Services, Information Policy Department of Ministry of Industry and Trade of Japan, 2004.

[4] A. Rechtschaffen and A. Kales, *A Manual of Standardized Terminology, Techniques and Scoring System for Sleep Stage of Human Subjects*. Washington, DC: Public Health Service U.S. Gov. Printing Office, 1968.

[5] B. H. Jansen and W.-K. Cheng, "Classification of sleep patterns by means of Markov modeling and correspondence analysis," *IEEE Trans. Pattern Anal. Mach. Intell.*, vol. 9, no. 5, pp. 707–710, Sep. 1987.

[6] I. Gath and A. B. Geva, "Unsupervised optimal fuzzy clustering," *IEEE Trans. Pattern Anal. Mach. Intell.*, vol. 11, no. 7, pp. 773–780, Jul. 1989.

[7] K. Otsuka and Y. Yanaga, "Studies of arrhythmias by 24 hours polygraphic recordings relationship between the heart rate and sleep stages," *Fukuoka Acta Med.*, vol. 72, no. 10, pp. 596–598, Oct. 1981.

[8] T. Salmi and L. Leinonen, "Automatic analysis of sleep records with static charge sensitive bed," *Electroencephalography Clin. Neurophysiol.*, vol. 64, no. 1, pp. 84–87, Jul. 1986.

[9] S. Doi and H. Takahashi, "Development of estimation method of sleep condition from information of human body movement by a neural network," *IEEJ*, vol. C-114, no. 11, pp. 84–87, 1994.

[10] R. H. Harper, V. L. Schechman, and K. A. Kluge, "Machine classification of infant sleep stage using cardio respiratory measures," *Electreoncephalography Clin. Neurophysiol.*, vol. 67, no. 4, pp. 379–387, Oct. 1987.

[11] Y. T. Peng, C. Y. Lin, M. T. Sun, and C. A. Landis, "Multimodality sensor system for long-term sleep quality monitoring," *IEEE Trans. Biomed. Circuits Syst.*, vol. 1, no. 3, pp. 217–227, Sep. 2007.
[12] W. Karlen, C. Mattiussi, and D. Floreano, "Sleep and wake classification with ECG and respiratory effort signals," *IEEE Trans. Biomed. Circuits Syst.*, vol. 3, no. 2, pp. 71–78, Apr. 2009.
[13] H. Watanabe and K. Watanabe, "Non-invasive measurement of heartbeat, respiration, snoring and body movement of a sleeping subject," *Trans. Soc. Instrum. Control Eng.*, vol. 35, no. 8, pp. 1012–1019, 1999.
[14] T. Watanabe and K. Watanabe, "Estimation of the sleep stages from the bio-data non-invasively measured in the sleep," *Trans. Soc. Instrum. Control Eng.*, vol. 38, no. 7, pp. 581–589, 2002.
[15] T. Watanabe and K. Watanabe, "Non-contact method for sleep stage estimation," *IEEE Trans. Bio-Med. Eng.*, vol. 51, no. 10, pp. 1735–1748, Oct. 2004.
[16] K. Watanabe, T. Watanabe, H. Watanabe, H. Ando, T. Ishikawa, and K. Kobayashi, "Noninvasive measurement of heartbeat, respiration, snoring and body movement of a subject in bed via a pneumatic method," *IEEE Trans. Bio-Med. Eng.*, vol. 52, no. 12, pp. 2100–2107, Dec. 2005.
[17] K. Watanabe, T. Manabe, and T. Yoshikawa, "Definition of sleep indices by pulse wave and body movement and estimation of sleep stages," *Trans. Soc. Instrum. Control Eng.*, vol. 42, no. 4, pp. 404–410, 2006.
[18] The Japanese Society of Sleep Research, Handbook of Sleep Science and Sleep Medicine, Tokyo, Japan: Asakura Publ. Comp., 1998.
[19] R. L. Williams, I. Karacan, and V. J. Hursch, "Electroencephalography (EEG) of human sleep," in *Clinical Applications*. Hoboken, NJ: Wiley, 1974.
[20] H. W. Agnew, Jr., W. W. Webb, and R. L. Williams, "Clinical and laboratory notes, sleep patterns in late middle age males: An egg study," *Electreoncephalography Clin. Neurophysiol.*, vol. 23, no. 2, pp. 168–171, Aug. 1967.
[21] Ono, Endo, Nishihara, Maki, and Koga, "Change in sleep by aging—Sleeps elder subjects then 60-," *Clin. Neurol.*, vol. 28, no. 2, pp. 88–93, 1986.
[22] Y. Hayashi, "Midnight polygraph (No. 2)—REM and slow wave sleeps," *Clin. Neurol.*, vol. 19, no. 10, pp. 660–668, 1979.
[23] *The AASM Manual for the Scoring of Sleep and Associated Events: Rules, Terminology and Technical Specification*, 2007.

Yosuke Kurihara received the M.E. and Ph.D. degrees from Hosei University, Tokyo, Japan, in 2003 and 2009, respectively.

Since 2009, he has been an Assistant Professor with the Department of Computer and Information Science, Faculty of Science and Technology, Seikei University, Tokyo. His research interests include sensor method and biosensing.

Dr. Kurihara is a member of Japanese Society for Medical and Biological Engineering, etc.

Kajiro Watanabe (M'01) received the M.E. and Ph.D. degrees from Tokyo Institute of Technology, Tokyo, Japan, in 1970 and 1973, respectively.

Since 1985, he has been a Professor with the Department of Advanced Sciences, Faculty of Science and Engineering, Hosei University, Tokyo, where he was a Research Assistant from 1973 to 1974, a Lecturer in 1975, and an Assistant Professor from 1950 to 1984. From 1980 to 1981, he was a Visiting Associate Professor with Oakland University, Rochester, MI, and from 1981 to 1982, he was the Research Associate with The University of Texas, Austin. In the industrial field, he acts as an authorized Japan Professional Engineer. He is the Chief Researcher of the several projects conducted by the Ministry of Economy, Trade, and Industry, Japan. His major interest is control and instrument, and he is currently interested in biomeasurement, sports measurement, robotics, fault diagnosis, vehicle, environmental monitoring, and intelligent control. He is the holder of 61 patents, has 12 publications in the control-engineering field, and has more than 230 referenced journals and conference proceedings.

Dr. Watanabe is a member of the Society of Instrument and Control Engineers.